Semiclassical Approach to Long Time Propagation in Quantum Chaos: Predicting Scars

Eduardo G. Vergini

Departamento de Física, Comisión Nacional de Energía Atómica., Avenida del Libertador 8250, (C1429BNP) Buenos Aires, Argentina

Escuela de Ciencia y Tecnología, Universidad Nacional de General San Martín, Alem 3901, (B1653HIM) Villa Ballester, Argentina

(Received 30 January 2012; published 26 June 2012)

We present two powerful semiclassical formulas for quantum systems with classically chaotic dynamics, one of them being the Fourier transform of the other. The first formula evaluates the autocorrelation function of a state constructed in the neighborhood of a short periodic orbit, where the propagation for times greater than the Ehrenfest time is computed through the contribution of homoclinic orbits. The second formula evaluates the square of the overlap of the proposed state with the eigenstates of the system, providing valuable information about the scarring phenomenon. Both expressions are successfully verified in the Bunimovich stadium billiard.

DOI: 10.1103/PhysRevLett.108.264101 PACS numbers: 05.45.Mt, 03.65.Sq, 05.45.Ac, 05.45.Pq

The method of semiclassical propagation is performed by associating quantum states with Lagrangian manifolds [1] in phase space, and the propagation is accomplished by the evolution of manifolds [2]. Furthermore, the semiclassical overlap of these states consists of an integration over the set of submanifolds resulting from the intersection of Lagrangian manifolds. Within this geometrical framework, the famous Van Vleck propagator is clearly understood [3]. This propagator is the starting point of practically all theoretical developments in quantum chaos, the Gutzwiller trace formula [4] being an outstanding example. Nevertheless, it suffers from three serious drawbacks. First, the Lagrangian manifolds used are not time invariant; this fact is very disappointing because the classical calculation must be repeated for all times involved. Second, the determination of each submanifold is a hard geometrical problem. Third, the number of submanifolds increases exponentially for times greater than the Ehrenfest time, this being a consequence of the chaotic nature of the dynamics.

We eliminate the first two drawbacks mentioned above by using a special quantum state, $|\gamma\rangle$, living in the neighborhood of an arbitrary short periodic orbit, γ [5]. This state is constructed in such a way that all the points of the periodic orbit are semiclassically equivalent; we could think of a tube in phase space enclosing γ, and with constant cross section from a symplectic point of view. Then, the forward (backward) propagation of $|\gamma\rangle$ is described by stretching the tube along the unstable (stable) manifold of γ; for this reason, the required Lagrangian manifolds are the unstable and stable manifolds of γ, which are time invariant. Furthermore, finding the intersection of these manifolds is a simple task, it consists of the set of homoclinic orbits (HOs) of γ. In this respect, it is worth mentioning that by using useful homoclinic canonical invariants [6] the integration along HOs is trivial.

Here we find the autocorrelation function of $|\gamma\rangle$ through a sum of HO contributions. Moreover, its Fourier transform provides information about the scarring phenomenon [7]; specifically, it gives the scar intensities and their position in the energy spectrum. Certainly, this information is relevant for the analysis of recent observations in quantum dots, optical microcavities, optical fibers, and graphene sheets [8].

Semiclassical formulas.—The autocorrelation function of $|\gamma\rangle$, presented for two degrees of freedom chaotic Hamiltonians and evaluated for times satisfying $|t| < \tau$ (with τ an arbitrary value greater than the Ehrenfest time), results in

$$\langle\gamma|e^{(i/\hbar)(E_\gamma-\hat{H})t}|\gamma\rangle \simeq F(\lambda t) + \frac{\sqrt{\hbar}}{\lambda P}\sum_{t_A\le\tau}\frac{f(\lambda|t|-\lambda t_A)}{\sqrt{|L|A}}e^{i\alpha\mathrm{sgn}(t)}, \quad (1)$$

where the phase α and the semiclassical time t_A are given by $\alpha = (S/\hbar - \mu\pi/2)$ and $t_A = \log(A/\hbar)/\lambda$, with E_γ the Bohr-Sommerfeld energy of $|\gamma\rangle$, P the period of γ, and λ its stability index. The sum runs over HOs of γ, and each HO (evaluated at energy E_γ) has four canonical invariants [6]: the homoclinic action S, the homoclinic Maslov index μ, the relevance A, and the normalized Lazutkin invariant L. S and A have units of action while L, being a ratio of actions, has no units. Finally, the dimensionless real functions F and f are given by

$$F(x) = 1/\sqrt{\cosh(x)} \quad \text{and} \quad f(x) = \sqrt{2}e^{-x/2}K_0(e^{-x}),$$

with K_0 being the modified Bessel function of zero order [9].

The function $F(\lambda t)$ describes the autocorrelation of $|\gamma\rangle$ when interference at HOs is not included. On the other hand, the switching function $f(\lambda|t| - \lambda t_A)$ turns on the influence of a given HO when $|t|$ is around t_A, while for $|t|$ greater than $\sim t_A + 4/\lambda$ its influence decreases exponentially to zero [see Fig. 1(a)]. Notice that as a

 © 2012 American Physical Society

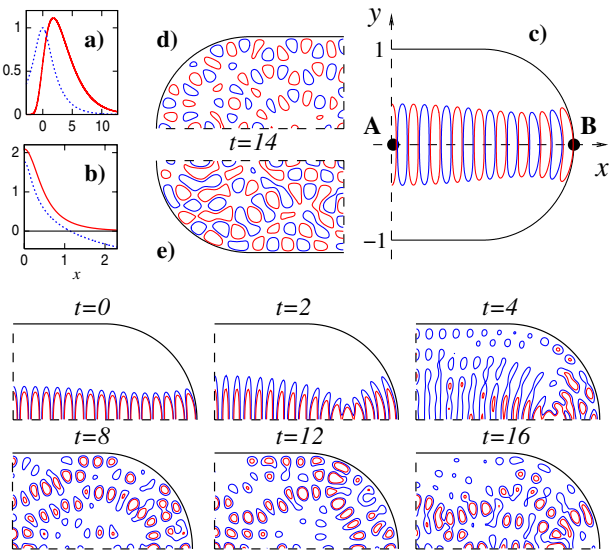

FIG. 1 (color online). (a) Switching function $f(x)$ (solid), and $F(x)$ (dashed). (b) Even functions $\tilde{F}(x)$ (solid) and $\eta(3x)/2$ (dashed). Contour lines at $\pm 0.4/\sqrt{2}$ of (c) $\varphi_{16}(x, y)$, (d) real part of an evolution of $\varphi_{16}(x, y)$, and (e) imaginary part of the same evolution. Also, contour lines at 0.5 and 1 of a sequence of propagated probability densities of $\varphi_{16}(x, y)$.

consequence of the switching function we only have to compute HOs with $t_A \lesssim |t|$.

The Fourier transforms of F and f ($\tilde{F}$ and $\tilde{f}$) are related by

$$\tilde{f}(x) = \sqrt{\pi/2}\tilde{F}(x)e^{ix\eta(x)}, \tag{2}$$

with $\tilde{F}$ and η [10] real even functions [see Fig. 1(b)]. Then, with E_ν and $|\nu\rangle$ the set of eigenenergies and eigenstates, and expanding $|\gamma\rangle$ in this basis, $|\gamma\rangle = \sum c_\nu|\nu\rangle$, one has after replacing Eq. (2) in the Fourier transform of Eq. (1)

$$\sum_\nu |c_\nu|^2 g(E - E_\nu) \simeq \tilde{F}\left(\frac{\omega}{\lambda}\right)\left(1 + \frac{\sqrt{2\pi\hbar}}{\lambda P}\sum_{t_A \lesssim \tau}\frac{\cos(\psi)}{\sqrt{|L|A}}\right), \tag{3}$$

with $g(E) = \sqrt{2/\pi}\hbar\lambda \sin(E\tau/\hbar)/E$, $\omega = (E - E_\gamma)/\hbar$, and $\psi = \eta(\omega/\lambda)\omega/\lambda + \omega t_A + \alpha$. The factor $\tilde{F}(\omega/\lambda)$ in Eq. (3) identifies those regions of the spectrum where γ is relevant [7], while the other factor (which mimics the Gutzwiller formula) provides a detailed description of the eigenstates influenced by γ; this influence was named *scarring* by Heller [7].

Resonances.—The state $|\gamma\rangle$ has a simple representation in configuration space by using local coordinates on γ [5,11]. The so-called resonance is the product of two functions: a local plane wave along γ, and a transverse wave packet that evolves according to a modified dynamics (we eliminate the contraction-expansion contribution to the motion in the vicinity of γ). After one turn around γ the wave packet accumulates the phase $S_\gamma/\hbar - \mu_\gamma\pi/2$, which is an integer multiple of 2π when the energy is E_γ, where S_γ and μ_γ are the action and Maslov index of γ. For billiards, explicit expressions are easily obtained [12]; in particular, the normalized even-even resonance of the horizontal periodic orbit in the Bunimovich stadium billiard with n nodes between $\mathbf{A}(x = 0, y = 0)$ and $\mathbf{B}(x = 2, y = 0)$ [see Fig. 1(c)] is given by [13]

$$\varphi_n(x, y) = N_n(x)e^{-[k_n y^2/2B(x)]}\cos[k_n x + g(x)k_n y^2/2 - \phi(x)/2], \tag{4}$$

where $B(x) = (1/a + ax^2)\cosh(2\lambda x) - 2x\sinh(2\lambda x)$, $g(x) = [ax\cosh(2\lambda x) - \sinh(2\lambda x)]/B(x)$, $N_n(x) = [k_n/\pi B(x)]^{1/4}$, and $\phi(x) = \mathrm{sgn}(x)\{\arctan[e^{2\lambda|x|}(a|x| - 1)/(a|x| + 1)] + \pi/4\}$, with $a = 1/\sqrt{2}$, $\lambda = \log(3 + \sqrt{8})/4$, the Bohr-Sommerfeld wave number $k_n = (n + 3/4)\pi/2$, and the function arctan(.) taking values in the range $(-\pi/2, \pi/2)$. In order to simplify the interpretation of the results, the velocity of the classical particle is taken as unity; in this way, the stability index λ has units of [length^{-1}], the period of the desymmetrized horizontal periodic orbit is $P = 4$ (the length going from **A** to **B** and back to **A**), $E_\gamma/\hbar = k_n/2$, and $\omega = (k^2 - k_n^2)/2k_n \sim k - k_n$.

Derivation.—The lhs of Eq. (1) is the overlap

$$(\langle\gamma|e^{(i/\hbar)(E_\gamma - \hat{H})t/2})(e^{(i/\hbar)(E_\gamma - \hat{H})t/2}|\gamma\rangle), \tag{5}$$

where the ket is a forward evolution (by $t/2$) of $|\gamma\rangle$ and the bra is a backward evolution (also by $t/2$) of $\langle\gamma|$. So, from a semiclassical point of view the ket (bra) is a state described by the unstable (stable) manifold of γ. The method used to evaluate overlaps between this type of semiclassical wave function was developed in Refs. [6,14]. The overlap consists of a term associated with the intersection of manifolds at the periodic orbit, plus a sum of contributions related to the intersection of manifolds at HOs. In the case of Eq. (5) one has for $t > 0$

$$\langle\gamma|e^{(i/\hbar)(E_\gamma - \hat{H})t}|\gamma\rangle \simeq F(\lambda t) + \sqrt{2\pi\hbar}\sum F_0(t)e^{i\alpha},$$

where $F_0(t)$ computes at time t the accumulated contribution to the amplitude of a given HO (see [6]),

$$F_0(t) = \frac{1}{P\sqrt{|L|}}\int_{-\infty}^{\infty} G(\sqrt{A}e^{\lambda t'}, t/2)G(\sqrt{A}e^{-\lambda t'}, t/2)dt', \tag{6}$$

with $G(q, t) = (\pi\hbar)^{-1/4}\exp(-q^2e^{-2\lambda t}/2\hbar - \lambda t/2)$ being a wave packet that evolves under the action of the quantum counterpart of the hyperbolic Hamiltonian λpq. Here the factor $G(\sqrt{A}e^{\lambda t'}, t/2)$ [$G(\sqrt{A}e^{-\lambda t'}, t/2)$] is the amplitude along the unstable (stable) manifold, and $\sqrt{|L|}$ is a nonlinear correction to the linear behavior produced by λpq. The integral in Eq. (6) is equal to $e^{-\lambda t/2}K_0(e^{-\lambda t}A/\hbar)/(\lambda\sqrt{\pi\hbar})$; then, by using the definitions of $f(x)$ and t_A we arrive at Eq. (1) for $t > 0$. For $t < 0$, the ket (bra) in the overlap lives on the stable (unstable) manifold, so the

phase α changes by $-\alpha$, and the integral in Eq. (6) is the same by replacing t with $-t$.

The Fourier transform of the left-hand side of Eq. (1) includes the window $|t| < \tau$ because the right-hand side goes immediately to zero for $|t| > \tau$. Moreover, the Fourier transform of F (and f) is not affected by such a window because τ is greater than λ^{-1}, the maximum time where $F(\lambda t)$ is relevant.

Classical tools.—The classical calculation is a simple task on a Poincaré surface of section. Here we use Birkhoff coordinates: q measures the position of a bounce on the desymmetrized boundary (see Fig. 2), and p is the fraction of momentum tangent to the boundary. The horizontal periodic orbit is represented by the fixed point **B** ($q = 1 + \pi/2$, $p = 0$), and its stable and unstable manifold directions by the vectors $\xi_s = 2^{-1/4}(-1, -1/\sqrt{2})$ and $\xi_u = 2^{-1/4}(-1, 1/\sqrt{2})$, normalized by the relation $\xi_u \wedge \xi_s = 1$. Then, a point on the unstable direction close to **B** is given by $\mathbf{B} + \epsilon\xi_u$ (with $|\epsilon| \ll 1$), and its forward evolution after κ steps on the section, $z = M^{\kappa}(\mathbf{B} + \epsilon\xi_u)$, lives on the unstable manifold (M is the map on the desymmetrized section). Moreover, we associate with z the parameter $u \simeq \epsilon e^{\kappa\lambda P}$ (with relative error ϵ) and then, one gets the vector $\xi_u(u) = dz/du$ tangent to the unstable manifold on the section (of course, $\xi_u(0) = \xi_u$). In the same way $\mathbf{B} + \epsilon\xi_s$ is a point on the stable direction close to **B**, and its backward evolution after κ steps, $z = M^{-\kappa}(\mathbf{B} + \epsilon\xi_s)$, lives on the stable manifold; in this case we associate with z the parameter $s \simeq \epsilon e^{\kappa\lambda P}$, obtaining the vector $\xi_s(s) = dz/ds$ tangent to the stable manifold on the section.

In Fig. 2 we calculate pieces of stable and unstable manifolds by taking $0 < \epsilon \leq 1/12$ and $\kappa = 3$ (notice that at $q = 0$ and $q = 1 + \pi/2$ manifolds change the sign of p). The intersection of these pieces of manifolds provides homoclinic points corresponding to 8 different HOs (with $\kappa = 4$, we find 56 HOs). The trajectories 4 and 5 are not time reversible, so each of them correspond to 2 HOs. The other trajectories, being time reversible, have one turning point (for instance, the points **a**, **c**, **e**, and **g** of trajectories 1, 6, 7, and 8).

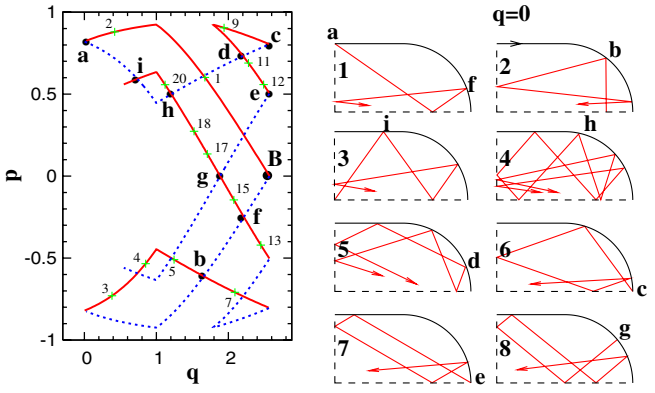

FIG. 2 (color online). Pieces of unstable (solid) and stable (dashed) manifolds of the horizontal periodic orbit (B) on the desymmetrized Poincaré surface of section in Birkhoff coordinates $q - p$. Some points on the unstable manifold with integer values of the parameter u are indicated with (+). The intersection of manifolds provides 8 HOs plotted on the right (the arrows indicate that they go asymptotically to the horizontal periodic orbit).

Invariants.—Here we discuss the evaluation of the canonical invariants used in Eqs. (1) and (3). Let z_0 be a homoclinic point with parameters u_0 and s_0. Then, the sequence of points $z_j = M^j z_0$ for j an integer, with parameters $u_j = e^{j\lambda P}u_0$ and $s_j = e^{-j\lambda P}s_0$, defines the HO on the Poincaré surface of section. Associated with the HO on the section one has

$$A_P = u_0 s_0 \quad \text{and} \quad L_P = \frac{\xi_u(u_0) \wedge \xi_s(s_0)}{\xi_u(0) \wedge \xi_s(0)};$$

L_P was introduced in Ref. [15] without including the denominator. These quantities take the same value for all the points of the sequence and, moreover, they are invariants with respect to canonical transformations on the section; however, they depend on the selected Poincaré surface of section. On the other hand, the relevance, A, and the normalized Lazutkin invariant, L, defined in Ref. [6] take the same value for all the points of the HO, being invariants with respect to general canonical transformations. The interesting point is that they can be evaluated on the section as follows

$$A = e^{\lambda T_D} A_P \quad \text{and} \quad L = e^{-\lambda T_D} L_P,$$

where $T_D = \sum(t_{j,j+1} - P)$ is a sum over the sequence of points, with $t_{j,j+1}$ being the time for going from z_j to z_{j+1}.

The homoclinic action and the homoclinic Maslov index are also evaluated over the sequence of points as $S = \sum(S_{j,j+1} - S_\gamma)$ [16] and $\mu = \sum(\mu_{j,j+1} - \mu_\gamma)$, where $S_{j,j+1}$ is the action for going from z_j to z_{j+1}, and $\mu_{j,j+1}$ is the corresponding angle swept by the unstable manifold direction divided by π. Here μ is equal to minus the number of bounces with the straight line of the stadium boundary [17]; for instance, $\mu = -1, 0, -2, -1, -1, 0, -2, -2$ for the HOs from 1 to 8 of Fig. 2. For completeness, we also provide approximated values of the other invariants as $(-S/(\hbar k_n), A/(\hbar k_n), L)$: (3.368, 1.4,1.0), (2.991, 1.7, −1.3), (5.952, 5.9,0.8), (5.908, 7.1, −1.0), (6.758, 4.0,1.7), (6.708, 3.3, −2.0), (6.917, 7.3, −1.1) and (6.565, 14.3, 0.9).

Numerical results.—The quantum calculation of the autocorrelation function is performed by expanding the resonance $\varphi_n(x, y)$ in the basis of even-even eigenfunctions, normalized to unity on the half stadium of Fig. 1(c). For the semiclassical calculation, to each HO of the quarter of stadium (see Fig. 2) corresponds two HOs of the half stadium [18]. So, the contribution of the trajectory number 1 (4) has to be included two (four) times in Eq. (1) [and Eq. (3)]. Figure 3 presents these calculations for 8 and 56

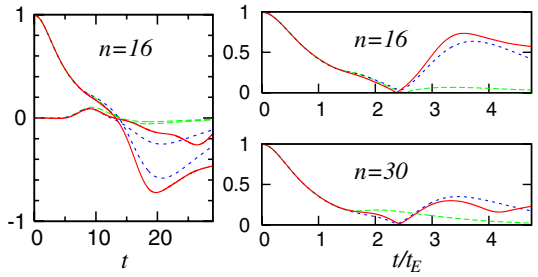

FIG. 3 (color online). Quantum calculation of the autocorrelation (solid), and its semiclassical approximation given by Eq. (1), with 8 HOs (dashed) and 56 HOs (short-dashed). On the left, the real and imaginary part as a function of t; for $t > 15$ the upper dashed line corresponds to the imaginary part. On the right, the modulus as a function of the time in units of the Ehrenfest time. n is defined in Eq. (4).

HOs, showing a satisfactory accord up to $2t_E$ and $3t_E$, respectively, where the Ehrenfest time is given by $t_E \sim \log(S_P/\hbar)/2\lambda = \log[(2+\pi)k_n]/2\lambda$, with S_P the area of the Poincaré section at energy E_γ.

Figure 4 displays $|c_\nu|^2$, the square modulus of the overlap of the resonance with the even-even eigenstate at wave number k_ν, as a function of $N(k_\nu)$. $N(k) = (1+\pi/4)k^2/(4\pi)$ provides the mean number of even-even eigenstates with wave number smaller than k (so, the mean level spacing is unity). These coefficients are compared with the semiclassical estimate given by the right-hand side of Eq. (3), which is normalized in such a way that the sum of the maxima is equal to one. The figure shows that 8 HOs are sufficient to predict the scarring intensities of the first 100 eigenstates, while 56 HOs improve the position of the maxima (see the case $n = 16$); of course, the error of the semiclassical prediction increases considerably for the smallest values of $|c_\nu|^2$.

Remarks and conclusions.—Our conclusions are as follows:

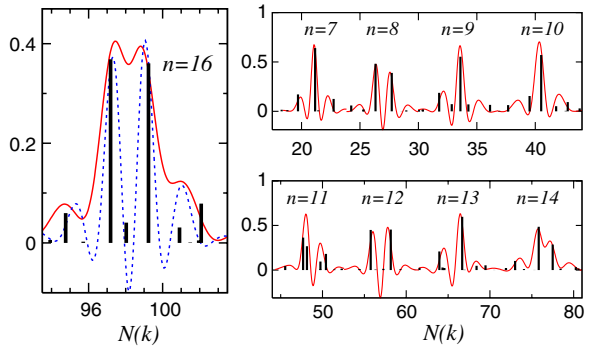

FIG. 4 (color online). Representation of $|c_\nu|^2$ as a function of $N(k_\nu)$ (vertical stick). The curves show the semiclassical approximation given by Eq. (3), with 8 HOs (solid) and 56 HOs (dashed). n is defined in Eq. (4).

(1) The semiclassical formula [Eq. (3)] is probably not convergent in the present form for the same reasons as the Gutzwiller is not; to answer this question it is necessary to establish the asymptotic behavior of the number of HOs as the relevance, A, increases. Then, to find eigenvalues up to the mean level spacing we should use resummation techniques as they were used to improve the convergency of the Gutzwiller formula [19]. Following this speculation and having in mind that our formalism puts the time and energy domains on equal footing, we believe that Eq. (1), improved with resummation techniques, ensures semiclassical propagation up to the Heisenberg time.

(2) The generalization to more than two degrees of freedom should be almost straightforward. Of course, it is necessary to generalize the defined homoclinic invariants. Moreover, the correlation function between states living on different periodic orbits should be treated in a similar way. In this case, it is necessary first to identify the relevant canonical invariants associated with heteroclinic motions.

(3) An evident application of Eq. (1) is the long time propagation of wave packets; this is performed by expanding the wave packet in a basis of resonances associated with a given periodic orbit. In this respect, in Ref. [20] there is an interesting numerical computation of the propagation of wave packets (in the stadium billiard) in terms of HOs; however, this calculation suffers from the same drawbacks as the Van Vleck formula.

(4) An interesting semiclassical criterion for scars in terms of periodic orbits was presented in Ref. [21]; however, it needs an enormous number of periodic orbits to find scars in the low energy spectrum (up to the first 100 eigenstates).

(5) Lagrangian manifolds have attracted an increasing interest in semiclassical developments. They were used to propagate wave packets up to the Ehrenfest time [22], and also to simplify the usual semiclasscial rules [23].

(6) The value of the invariant L depends on the nonlinearity of the manifolds in the vicinity of the HO. In the stadium, the highest values of L correspond to whispering-gallery HOs (5 and 6 of Fig. 2). In chaotic linear maps, $L = 1$.

Equation (1) shows the way to deal with long time dynamics. It is mandatory to use the stable and unstable manifolds of periodic orbits because they are time invariant. Furthermore, as the intersection of these manifolds consists of the set of homoclinic and heteroclinic orbits, it is also mandatory to find those canonical invariants that are able to capture the contribution of these orbits easily.

Equation (3) is the product of two factors. The first factor is related to the periodic orbit itself and only contains information of the short time dynamics, while the second factor incorporates the long time dynamics through the contribution of HOs. A remarkable point about this formula is that a few HOs are sufficient to provide relevant quantum information in the low energy spectrum.

[1] V. I. Arnold, *Mathematical Methods of Classical Mechanics* (Springer-Verlag, New York, 1984).
[2] V. P. Maslov and M. V. Fedoriuk, *Semi-Classical Approximation in Quantum Mechanics* (Reidel, Boston, 1981).
[3] R. G. Littlejohn, J. Stat. Phys. **68**, 7 (1992).
[4] M. C. Gutzwiller, *Chaos in Classical and Quantum Mechanics* (Springer, New York, 1990).
[5] E. G. Vergini, J. Phys. A **33**, 4709 (2000).
[6] E. G. Vergini, E. L. Sibert III, F. Revuelta, R. M. Benito, and F. Borondo, Europhys. Lett. **89**, 40013 (2010).
[7] E. J. Heller, Phys. Rev. Lett. **53**, 1515 (1984).
[8] Y. H. Kim, M. Barth, H. J. Stockmann, and J. P. Bird, Phys. Rev. B **65**, 165317 (2002); Q. H. Song, L. Ge, A. D. Stone, H. Cao, J. Wiersig, J. -B. Shim, J. Unterhinninghofen, W. Fang, and G. S. Solomon, Phys. Rev. Lett. **105**, 103902 (2010); C. Michel, V. Doya, O. Legrand, and F. Mortessagne, Phys. Rev. Lett. **99**, 224101 (2007); H. Liang, Y. -C. Lai, D. K. Ferry, R. Akis, and S. M. Goodnick, J. Phys. Condens. Matter **21**, 344203 (2009).
[9] M. Abramowitz and I. A. Stegun, *Handbook of Mathematical Functions* (National Bureau of Standards, Washington, DC, 1972).
[10] We use the estimate $\eta(x) \approx 3.534[1-(x/3.41)^2]/[1+2.81x^2-0.25x^4+0.06x^6]^{1/2}$.
[11] E. G. Vergini and G. G. Carlo, J. Phys. A **34**, 4525 (2001).
[12] E. G. Vergini and G. G. Carlo, J. Phys. A **33**, 4717 (2000).
[13] A didactic explanation is found in Chapter 5 of the book *New Directions in Linear Acoustics and Vibration,* edited by M. Wright and R. Weaver (Cambridge University Press, Cambridge, England, 2010).
[14] E. G. Vergini and D. Schneider, J. Phys. A **38**, 587 (2005); E. G. Vergini, D. Schneider, and A. M. F. Rivas, J. Phys. A **41**, 405102 (2008).
[15] V. G. Gelfreich, V. F. Lazutkin, and M. B. Tabanov, Chaos **1**, 137 (1991).
[16] A. M. Ozorio de Almeida, Nonlinearity **2**, 519 (1989).
[17] There is no contribution from bounces with the axes (Neumann condition). Moreover, as a bounce with the stadium boundary (Dirichlet condition) increases the Maslov index by 3 (2) when it occurs on the circle (straight line), then $\mu_{j,j+1}-\mu_\gamma=0(-1)$.
[18] Equations (1) and (3) do not directly work for the quarter of stadium because, in such a case, γ lives on the border.
[19] A. Voros, J. Phys. A **21**, 685 (1988); M. V. Berry and J. P. Keating, J. Phys. A **23**, 4839 (1990); P. Cvitanović and B. Eckhardt, Phys. Rev. Lett. **63**, 823 (1989).
[20] S. Tomsovic and E. J. Heller, Phys. Rev. E **47**, 282 (1993).
[21] O. Agam and S. Fishman, Phys. Rev. Lett. **73**, 806 (1994).
[22] R. N. P. Maia, F. Nicacio, R. O. Vallejos, and F. Toscano, Phys. Rev. Lett. **100**, 184102 (2008).
[23] J. Vanicek and E. J. Heller, Phys. Rev. E **64**, 026215 (2001).